hydrology

MDPI

Article

Long Term Historic Changes in the Flow of Lesser Zab River, Iraq

Rawshan Ali [1,2,*], Arez Ismael [3], Arien Heryansyah [4] and Nadeem Nawaz [5]

1 College of Hydraulic and Environmental Engineering, China Three Gorges University, Yichang 443002, Hubei, China
2 Department of Petroleum, Koya Technical Institute, Erbil Polytechnic University, Erbil 44001, Kurdistan, Iraq
3 Department of Architectural, Cihan University Campus/Sulaimaniya, Sulaimaniya 46001, Kurdistan, Iraq; Arez.ismael@sulicihan.edu.krd
4 Faculty of Engineering, Universitas Ibn Khaldun (UIKA), Bogor. Jalan KH Sholeh Iskandar KM.2, Kedung Badak, Tanah Sereal, Kota Bogor, Jawa Barat 16162, Indonesia; arengga@gmail.com
5 Faculty of Engineering Science and Technology, Lasbela University of Agriculture, Water and Marine Sciences, Uthal 90150, Pakistan; nn.engr96@yahoo.com
* Correspondence: rawshanothman@yahoo.com; Tel.: +86-155-4927-4896

Received: 21 January 2019; Accepted: 10 March 2019; Published: 13 March 2019

Abstract: The assessment of trends in river flows has become of interest to the scientific community in order to understand the changing characteristics of flow due to climate change. In this study, the trends in river flow of Dukan Dam located in the northern part of Iraq were assessed. The assessment was carried out for the period 1964 to 2013 using Sen's slope and the Mann–Kendall test. Sen's slope was used to assess the magnitude of change while the Mann–Kendall trend test was used to confirm the significance of trends. The results of the study showed that there was a decreasing trend in river flow both annually and for all individual months. The highest decreasing trend of -5.08846 m^3/month was noticed in April, while the lowest change of -1.06022 m^3/month was noticed in November. The annual flow also showed a significant decrease at a rate of -1.912 m^3/year at a 95% level of confidence. Additionally, the findings of the study also confirmed that a decrease in precipitation and the construction of hydraulic structures reduced the flow in the river. The findings of the study suggest that decreasing trends may cause a water-scarce situation in the future if proper adaptation measures are not taken.

Keywords: river flow trends; climate change; Mann–Kendall; Sens's slope; Iraq

1. Introduction

High concentrations of greenhouse gases are causing an increase in global temperature [1–4]. The increase in temperature is playing an adverse role in altering the components of the global hydrological cycle [5–9]. Precipitation is considered to be the most vigorous component of the global hydrological cycle, which has reportedly altered over several regions around the world [10–13]. The alteration of precipitation characteristics can have severe impacts on society in the form of floods and droughts, which can have an adverse impact on people's socio-economic situation [14–17]. Changes in streamflow or river flow are often associated with changes in precipitation. Cigizoglu, et al. [18] reported that stream flow changes are very sensitive to even small changes in precipitation. Therefore, it is very important and informative to investigate trends in river flow.

Trend assessments of river flow provide basic information related to water [18–25]. Several trend assessments have shown that changes in the characteristics of temperature and precipitation have direct impacts on river flows across the world [26–30]. Iraq, located in Asia, has also experienced

changes in precipitation and temperature in the last fifty years [31–33]. Therefore, it can be remarked that climate change may have impacted the water resources of Iraq. Additionally, Shubbar, Salman and Lee [33] reported that the temperature in Iraq will increase in future. Future temperature increases will modify precipitation patterns, which will affect the major water reservoirs. Thus, it is important to evaluate the trends in the major water reservoirs of Iraq. Knowledge of the changes in river flow in Iraq is very limited due to the availability and quality of data [31]. However, it is one of the most water stressed countries in the region. The gradual decline of water resources due to a decline in rainfall has been reported in Iraq [32]. This reinforces the need for a quantification of the changes in river flow in the country. Such analysis should be conducted with robust statistical methods considering the quality of data and missing values. The present study considered non-parametric methods that can provide trends and their significance when data quality is doubtful.

A number of dams have been constructed in the northern region of Iraq, such as in Mosul, Duhok, and Dukan. Dukan Dam, constructed over the lower Zab catchment is playing a vital role in supplying water to a large population in Iraq [34,35]. However, in recent years changes in the characteristics of precipitation have been reported over the region, which is expected to have an impact on the flow of the river [32,36]. Therefore, it is important to evaluate trends in the flow of Dukan Dam in order to avoid major crises regarding water supply in the region in the future. A review of the literature revealed that no studies has evaluated the river flow trends in the Dukan Dam flow. Thus the major objective of the study was to assess the long-term historic trends in the flow of the Lesser Zab river.

A number of trend assessment procedures are available in the literature, such as linear regression, Bayesian, and Mann–Kendall tests [37,38]. The Mann–Kendall test is considered to be a robust method for trend assessment and is also recommended by the World Meteorological Organization [39–41]. Thus, in this study the Mann–Kendall trend test was used for the confirmation of trends in the river flow (monthly, mean annual, annual maximum and annual minimum flows). The least square and Sen's slope tests are most widely used for estimating the magnitude of a trend. However, Sen's slope is not influenced by extreme values and thus is more robust compared to other methods. Thus, in this study, Sen's slope was used to estimate the magnitude of the change in trends. The assessment was carried out on data from fifty years ranging from 1964 to 2013.

2. Study Area and Datasets

Dukan Dam (Figure 1) is a multi-purpose cylindrical concrete arch dam located in the northern regions of Iraq (latitude: 35°57′15″ N and longitude: 44°57′10″ E) [42]. The dam is 360 m long, 116.5 m high, and 34.3 m and 6.2 m wide at the base and crest, respectively. The dam has a catchment size of 11,690 km^2, with a surface area of 270 km^2. The normal operational level of the dam is 511 m above the mean sea level. The dam was constructed across the Lesser Zab in 1954 to ensure water supply to the population for domestic, industrial and agricultural purposes [42,43]. The dam is now also used for controlling floods and power generation [44]. The dam has the capacity to impound 6,100,000,000 m^3 of water with two spillways, i.e., a tunnel and a bell-mouth. The tunnel is used to discharge excess water while the bell-mouth is operated during emergency periods. One of the major advantages of the reservoir is its capacity and gravel type bed, which helps to increase the water level in the area.

The study area experiences two climatic seasons, summer and winter. Summer begins in June and lasts until September, while winter begins in November and lasts until March. Around 90% of the rainfall occurs from November to April, and the rest of the months are mostly dry [32]. Rainfall in the area varies from 200 mm to 1000 mm [35]. The land use/land cover of the study area is mainly characterized by winter plants and pastures (82.7%), forest (15.6%), vegetables (1.6%) and urban areas (0.1%) [42].

The monthly river flow data recorded at two gauging stations were acquired from the Directorate of Dukan Dam. The data was collected for the period 1964 to 2013. The percentage of missing data was found to be 0.67% (upstream side) and 2.83% (downstream side) of the dam. Missing values in any dataset can be estimated by various statistical methods, for example, arithmetic averaging [45], inverse

distance interpolation [46], multiple regression analysis [47], closest station method [48], artificial neural network [49,50] and expectation maximization (EM) algorithm [51]. In this study, missing data were filled using the EM approach [52]. EM has been widely used in recent years for filling missing data in hydro-climatological records [53,54]. The completed data series were arranged in Excel for further analysis. The monthly flow of each year was used to compute the mean annual, annual maximum and annual minimum flow.

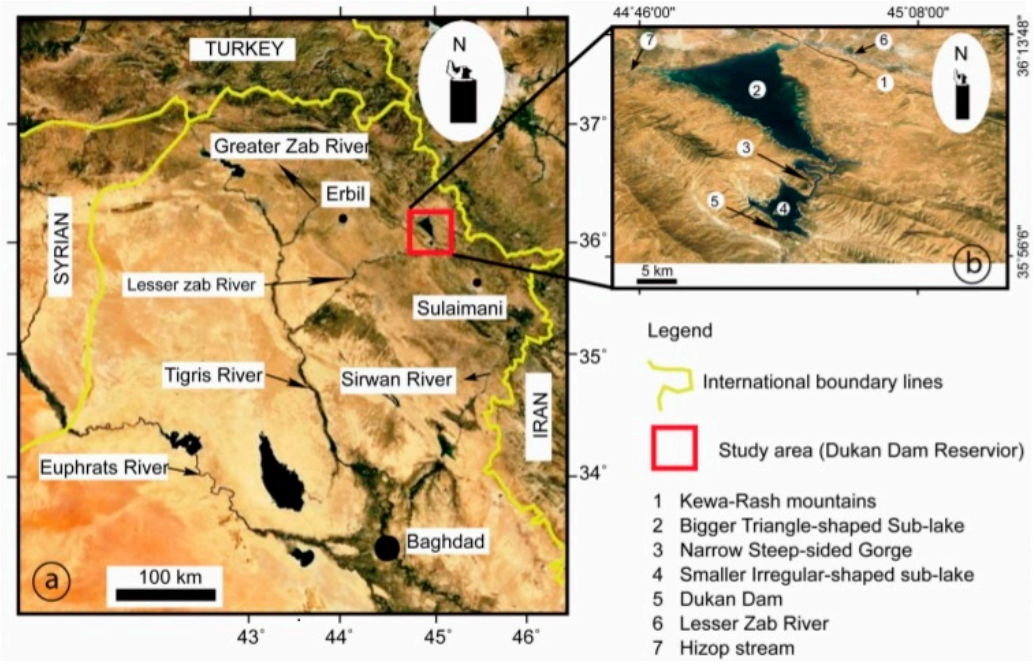

Figure 1. Location map of the Dukan Dam Reservoir. (**a**) Iraq map shows the main rivers in Iraq the location of the Dukan Dam Reservoir. (**b**) A photo taken from Google Earth showing the geographic location, the main rivers feeding the reservoir and its division into two sub-reservoirs (adapted from [43]).

3. Methodology

3.1. Distributional Analysis

Distributional analyses are frequently performed on hydrological studies to understand the nature of the data [55]. A number of frequency distribution methods are available in the literature such as normal, log normal, uniform, generalized extreme value, binomial, gamma, etc. In the present study, gamma, generalized extreme value and normal distributions, which are widely used in hydro-climatic studies, were applied to the datasets of Dukan Dam. The gamma and generalized extreme value are widely used for fitting skewed data, which is often noticed in hydrological data [55]. In addition, normal distribution was used as monthly river flow was often found to follow such a distribution. The goodness of fit for the tests was assessed using the Kolmogorov–Smirnov (KS) test. The KS test is found to be more powerful than the Anderson–Darling and Chi-square test [55]. Therefore, the test was applied for each month, mean annual flow, annual maximum flow and annual minimum flow at a 95% level of confidence with a null-hypothesis. Therefore, the test was applied for each month, mean annual flow, annual maximum flow and annual minimum flow at a 95% level of confidence with a null-hypothesis of the data followed the particular distribution (gamma, generalized extreme value and normal distribution).

3.2. Estimation of Magnitude of Change

In this study, Sen's slope [56] method was applied to calculate the intensity of the change in river flow. The method is non-parametric and calculates the slope with a pair of equal data. The method is well-known and widely used for the calculation of trends [23,24,57]. The slope of a trend can be calculated using the following equation:

$$Q = \frac{x_j - x_k}{j - k} \text{ For i } = 1, 2, 3, \ldots\ldots, n \tag{1}$$

where x_j and x_k are the data values at times j and k, (j > k), respectively. The median of these *N* values of Q is Sen's slope. If there is only one data in each time period, then:

$$N = n(n-1)/2 \tag{2}$$

where *n* is the number of periods. The median of the *N* estimated slopes is obtained in the usual way, the N values of Q are ranked by $Q_1 \leq Q_2 \leq \cdots \leq Q_{N-1} \leq Q_N$ and is estimated as below:

$$Q = \begin{cases} Q([(n+1)/2]) \text{ifnisodd} \\ \frac{Q_{[n/2]} + Q_{[(n+2)/2]}}{2} \text{ifniseven} \end{cases} \tag{3}$$

3.3. Mann–Kendall Trend Tests

The Mann–Kendall test was used to reveal the trends in monthly and mean annual, annual maximum and annual minimum river flow data [18,58,59]. The Mann–Kendall test (MK) is frequently used for trend assessment and is a nonparametric test [60]. The test is also endorsed by the World Meteorological Organization (WMO) for hydro-meteorological trend assessments. The MK test has the ability to handle outliers and it is distribution free [16,38,61]. Mann–Kendall test statistics (*S*) for river flow series can be calculated as:

$$S = \sum_{i=2}^{n} \sum_{j=1}^{i-1} \text{Sign}\left(x_i - x_j\right) \tag{4}$$

In Equation (4), n is data length, and x_i and x_j are sequential data in series, while the sign is calculated as below:

$$\text{sign}\left(x_i - x_j\right) = \begin{cases} -1 \text{for } \left(x_i - x_j\right) < 0 \\ 0 \text{for} \left(x_i - x_j\right) = 0 \\ 1 \text{for} \left(x_i - x_j\right) > 0 \end{cases} \tag{5}$$

The variance of the statistic can be calculated as:

$$V_o(S) = \frac{s(n-1)(2n+5) - \sum_{P-1}^{q} tp\left(t_p - 1\right)\left(2t_p + 5\right)}{18} \tag{6}$$

In Equation (6), t_p refers to ties of the p_{th} value, and q refers to a tied values number. Standardized test statistics for the Mann–Kendall test can be calculated as:

$$\mu_1 = \begin{cases} \frac{s-1}{\sqrt{\text{Var}(S)}} \text{ if } S > 0 \\ 0 \text{ if } S = 0 \\ \frac{s+1}{\sqrt{\text{Var}(S)}} \text{ifS} < 0 \end{cases} \tag{7}$$

Positive and negative μ_1 values indicate that the direction of the trend exists in a time series.

4. Result and Discussion

4.1. Distributional Analysis

Gamma, generalized extreme value and normal distribution were individually applied to the data for each month, the mean annual, annual maximum, and annual minimum flow. Tests were applied to the data of both gauges located on the upstream and downstream side of the dam at 95% level of confidence. The obtained results are presented in Table 1. Bold values in the table show that the hypothesis is rejected at the 95% level of confidence, while values in italic indicate the best fit. As can be seen in Table 1, the null hypothesis was accepted for most of the months in all tests. In the upstream side gauge, all data was found to follow the gamma and generalized extreme value distributions, while the null hypothesis was rejected in the month of March for the normal distribution. On the other hand, for the downstream side gauge all data was found to follow the generalized extreme value distribution. In the gamma distribution, the months of March, April, May and the annual maximum flow were found to show a rejected null hypothesis. Similarly, in the normal distribution, the months of January, March, April, May and the annual maximum flow were rejected. Overall, the generalized extreme value was found to have the best fit for the Dukan Dam data.

Table 1. Kolmogorov–Smirnov test statistics obtained during the fitting distribution of river flow on the upstream and downstream side gauge data of the dam.

Month/Season	Upstream Gauge			Downstream Gauge		
	Gamma	Gen. Extreme Value	Normal	Gamma	Gen. Extreme Value	Normal
Jan	*0.071*	0.072	0.150	*0.136*	0.146	**0.190**
Feb	*0.063*	0.067	0.118	*0.065*	0.071	0.151
Mar	0.123	*0.092*	**0.202**	**0.207**	*0.113*	**0.232**
Apr	*0.051*	0.063	0.103	**0.325**	*0.071*	**0.276**
May	0.089	*0.076*	0.142	**0.253**	*0.077*	**0.285**
Jun	0.082	*0.073*	0.153	0.109	*0.065*	0.142
Jul	0.093	*0.074*	0.139	0.089	*0.080*	0.130
Aug	0.115	*0.105*	0.127	0.128	*0.103*	0.120
Sep	0.098	*0.076*	0.096	0.130	*0.097*	0.101
Oct	*0.071*	0.072	0.150	0.139	*0.071*	0.078
Nov	0.153	0.096	*0.090*	0.088	*0.065*	0.095
Dec	0.090	*0.055*	0.184	0.131	*0.088*	0.092
Mean Annual	0.095	*0.085*	0.116	0.107	*0.097*	0.121
Maximum Flow	0.109	*0.081*	0.141	**0.203**	*0.122*	**0.216**
Minimum Flow	0.152	0.103	*0.088*	0.095	*0.085*	0.180

4.2. Seasonal Distribution of Flow

The seasonal distribution of monthly flow in the Dukan Dam is shown in Figure 2. Figure 2 shows the monthly distribution of the changes recorded at the station located before the Dukan reservoir. The figure clearly shows that flow was high in the months of December to May and relatively low in the months of June to November. The highest flow can be seen in the month of July, while the lowest was recorded in the month of September. The month of April showed a flow of around 450 m^3/sec, while the flow was around 50 m^3/sec during September. It is also clear from Figure 2 that the months of August to October had more or less the same flow, which was around 50 m^3/sec. It is also clear from Figure 2 that the flow increased from December to April and then started to decline. This change from increase to decrease was due to the rainfall over the region during that period.

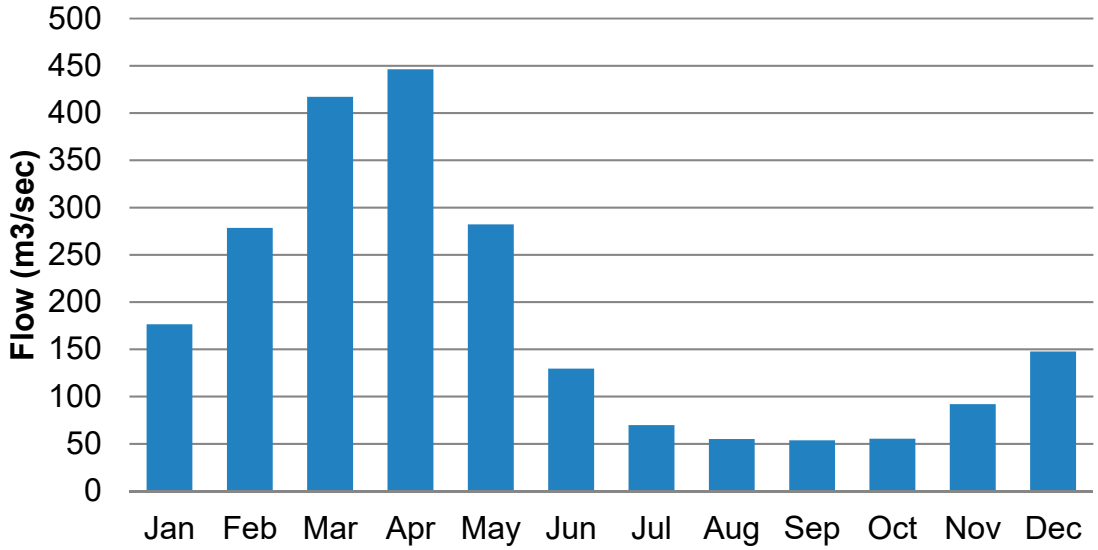

Figure 2. Seasonal distribution of flow recorded before Dukan Dam.

The seasonal distribution of the monthly flow recorded after Dukan Dam is shown in Figure 3. The figure shows that flow was highest in the month of August and lowest in April. Overall, most of the months had a flow of more than 100 m^3/sec. It can be noted that flow started to rise from the month of July and onwards, which is contradictory to the flow before the dam, where the flow started decreasing from the month of July. The increases in flow were due to the surplus water from the reservoir and also in order to maintain a minimum flow in the river. It is also clear from Figures 2 and 3 that the flow was high from the months of January to May upstream and low from June to December on the downstream side of the dam.

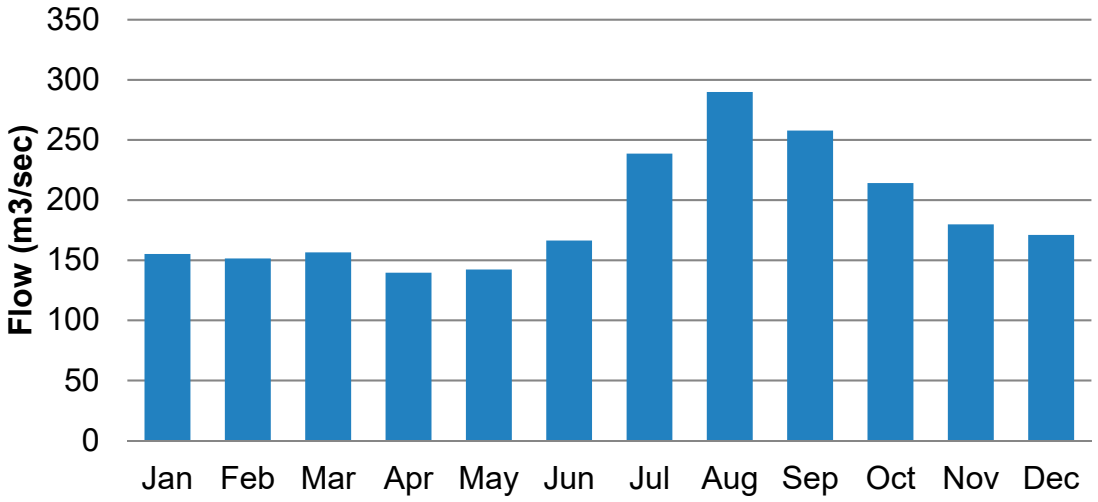

Figure 3. Seasonal distribution of flow recorded after Dukan Dam.

4.3. Trends in Monthly and Annual Flow

The magnitude of trends in river flow was assessed using Sen's slope while the significance was confirmed using the Mann–Kendall trend test. Sen's slope and the Mann–Kendall trend test were individually applied to each month and the mean annual flow for the period 1964 to 2013. The obtained results for the upstream and downstream side gauges are presented in Table 2. Table 2 shows the Z statistic, significance at the 90% and 95% levels of confidence and the change in each month and mean year. Table 2 shows that there were significant increases and decreases in trends on both sides of the dam. In the upstream gauge, the months of April, May, November and December showed significant

trends. The trends in April, May, November were significant at the 95% level of confidence, while the trends in December were found to be significant at the 99% level of confidence. It is important to mention here that annual flow also had a negative significant trend at the 90% level of confidence. The highest significant trend of −5.08846 m^3/year was observed for the month of April, followed by −2.70121 m^3/year in the month of May. On the other hand, the trend in mean annual river flow showed a change of −1.912 m^3/year at the 90% level of confidence. It also can be noted that none of the month or mean annual flows have shown an increasing trend. A decrease in river flow trends has also been observed in other parts of the world, such as Turkey [18] and Canada [22].

Similar to the upstream side gauge, the downstream side gauge station also showed a decrease in flow in all months except June, where a change of 0.73651 m^3/sec was recorded. It can be noted that the highest decrease (−4.3828 m^3/sec) was recorded in the month of September, followed by October (−3.7975 m^3/sec). It is also important to note that the changes were not significant in both months. A significant change was observed in the months of January, February, March, April, August, November and December. Most of the months were significant at the 90% level of confidence. The trends in the month of August and the mean annual flow were found to be significant at the 95% level of confidence. It is interesting to note that the flow for the month of December significantly decreased on both sides of the dam at the 99% level of confidence.

Table 2. Trends in monthly and mean annual river flow obtained using Sen's slope and Mann–Kendall trend test located up- and down-stream of Dukan Dam.

Time Series	Upstream Gauge			Downstream Gauge		
	Test Z	Significance	Q	Test Z	Significance	Q
Jan	−1.44		−1.31	−2.27	*	−1.6019
Feb	−1.07		−1.65	−2.36	*	−2.0343
Mar	−1.42		−2.67	−2.28	*	−1.5108
Apr	−2.38	*	−5.09	−2.22	*	−1.2254
May	−2.48	*	−2.70	−1.36		−0.6374
Jun	−3.58		−2.02	0.77		0.73651
Jul	−4.89		−1.33	−0.45		−0.3925
Aug	−6.74		−1.41	−2.87	**	−2.495
Sep	−6.51		−1.57	−4.32		−4.3828
Oct	−5.25		−1.31	−4.05		−3.7975
Nov	−2.48	*	−1.06	−2.35	*	−2.0692
Dec	−1.66	+	−1.17	−1.94	+	−1.7103
Annual	−2.59	**	−1.91	−2.91	**	−1.8038

*, ** and + represents significance at 90%, 95% and 99% confidence level.

4.4. Trends in Maximum Annual Flow

The trends in maximum flow assessed at the upstream (a) and downstream (b) side gauges are shown in Figure 4. The trends were assessed based on the maximum flow recorded for each month. The figure shows that flow had a decreasing trend on both sides of the dam. The trend estimated using Sen's slope showed a negative change of −4.073 m^3/sec/year on the upstream side, which was also found to be significant at the 99% confidence level. On the other side of the dam, the flow was also found to have decreased. The decrease rate was recorded as −2.540 m^3/sec and was significant at the 90% level of confidence. It is important to note that there was a decrease in the maximum flow on the upstream side of the dam, which indicates that the decrease in precipitation resulted in a decrease in the maximum flow. A decrease in precipitation was also reported in the study by Salman, et al. [62] and the study by Shubbar, Salman and Lee [33]. Besides the reduction in precipitation, the media also reported that the construction of Garan Dam in Iran, which is near Dukan Dam, has also reduced the flow. Additionally, Hassan, et al. [63] reported that the construction of hydrological schemes in the

catchment has reduced the flow in Dukan Dam. Overall, the decrease in maximum flow was relatively higher in recent years on both sides of the dam.

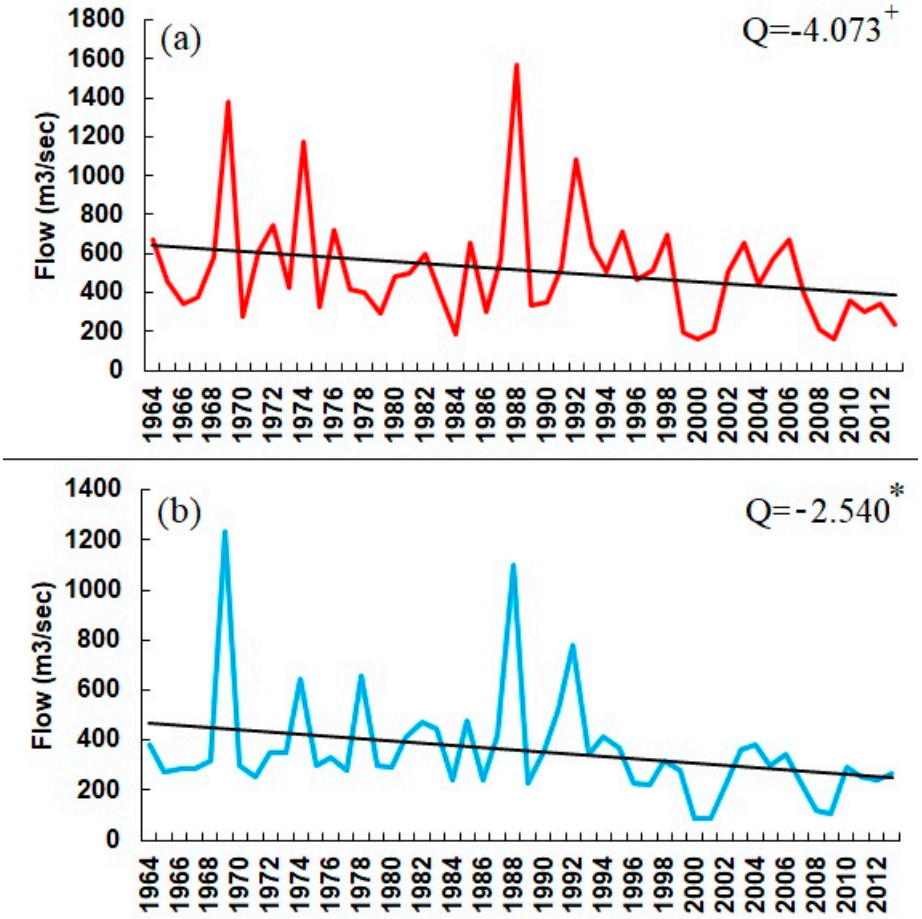

Figure 4. Trends in the maximum annual river flow on the (**a**) upstream and (**b**) downstream sides of Dukan dam.

4.5. Trends in Minimum Annual Flow

The trends in the minimum flow on both sides of the dam were also assessed. The assessment was performed based on the minimum values recorded each year. The obtained results are displayed in Figure 5. The figure clearly shows that there was a decrease in flow on both sides of the dam. However, the decrease was relatively higher on the upstream side of the dam. The Sen's slope estimated a negative change of -1.082 m^3/sec, while the Mann–Kendall trend test did not show any significance at the 90%, 95% or 99% confidence level. Similar to the upstream side, the downstream side showed a negative change of -0.948 m^3/sec. The negative change in the downstream side of the dam was found to be significant at the 95% confidence level. It is also important to note the minimum flow was higher on the downstream side compared with upstream. This could be due to the dependence of flow or discharge from the reservoir.

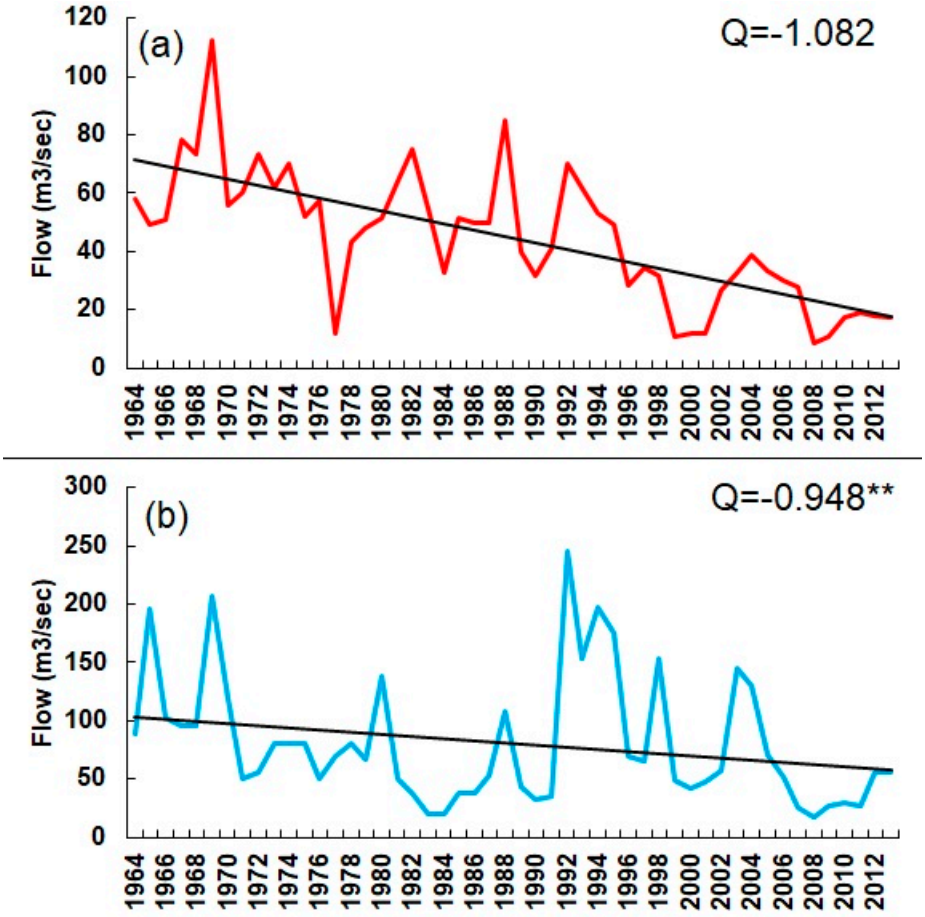

Figure 5. Trends in the minimum annual river flow on the (**a**) upstream and (**b**) downstream sides of Dukan dam.

5. Conclusions

This study presented the distributional analysis results, and trends in the monthly, mean annual, annual maximum and annual minimum flow of Dukan Dam located in the northern region of Iraq. The trends were assessed for the period 1964 to 2013. The rate of change in the river flow was assessed using Sen's slope, and the Mann–Kendall trend test was used to confirm the significance of the trends. The results of the study showed that the generalized extreme value trend fit best with the flow data of Dukan Dam. The results of the trend analysis showed that river flow was significantly decreased in all months on both sides of the dam. The month of April showed the highest rate of change upstream, while September showed the highest rate of change on the downstream side of the dam. The month of November and July showed the lowest change in the upstream and downstream sides of the dam, respectively. Significant changes were noticed in the months of April, May, November and December. Similarly, changes in the annual river flow were also found to be significant. Negative significant changes were also noticed in the maximum and minimum flow on both sides of the dam. The maximum flow was found to have decreased relatively significantly on the upstream side of the dam, which indicates a decrease in precipitation. In addition, the construction of hydraulic structures can be a major cause of the reduction in flow. It is expected that the findings of this study will help in the planning and management of the agriculture and water resources of Dukan region.

It can be noted that the results presented in this study are based on the standard Mann–Kendall trend test. In recent years, it has been reported that long-term persistence or the Hurst phenomenon influence the variance of test statistics and can alter the significance of the results acquired using the assumptions of independence and short-term persistence. Therefore, in the future, modified versions

of the Mann–Kendall trends can be used to confirm the influence of long-term persistence or the Hurst phenomenon on the significance of trends. Additionally, the present study was conducted using 30 years of data. In the future, studies can be conducted using a more recent and longer period of data. Furthermore, more stations can be incorporated to understand the overall changes in the catchment.

Author Contributions: R.A. and A.I. designed the research and wrote the manuscript. A.H. and N.N. critically reviewed the paper.

Funding: The authors wish to sincerely thank the China Scholarship Council, China Three Gorges University for funding this study.

Acknowledgments: We are grateful to the Directorate of Dukan Dam for providing data.

Conflicts of Interest: The authors declare no conflict of interest.

References

1. Karl, T.R.; Trenberth, K.E. Modern Global Climate Change. *Science* **2003**, *302*, 1719–1723. [CrossRef]
2. Crawford, J.; Venkataraman, K.; Booth, J. Developing climate model ensembles: A comparative case study. *J. Hydrol.* **2019**, *568*, 160–173. [CrossRef]
3. Ahmed, K.; Chung, E.-S.; Song, J.-Y.; Shahid, S. Effective Design and Planning Specification of Low Impact Development Practices Using Water Management Analysis Module (WMAM): Case of Malaysia. *Water* **2017**, *9*, 173. [CrossRef]
4. Moazenzadeh, R.; Mohammadi, B.; Shamshirband, S.; Chau, K.-W. Coupling a firefly algorithm with support vector regression to predict evaporation in northern Iran. *Eng. Appl. Comput. Fluid Mech.* **2018**, *12*, 584–597. [CrossRef]
5. Stagl, J.; Mayr, E.; Koch, H.; Hattermann, F.F.; Huang, S. Effects of climate change on the hydrological cycle in central and eastern Europe. In *Managing Protected Areas in Central and Eastern Europe Under Climate Change*; Springer: Dordrecht, The Netherlands, 2014; pp. 31–43.
6. Wang, Y.; Wang, D.; Lewis, Q.W.; Wu, J.; Huang, F. A framework to assess the cumulative impacts of dams on hydrological regime: A case study of the Yangtze River. *Hydrol. Process.* **2017**, *31*, 3045–3055. [CrossRef]
7. Iqbal, Z.; Shahid, S.; Ahmed, K.; Ismail, T.; Nawaz, N. Spatial distribution of the trends in precipitation and precipitation extremes in the sub-Himalayan region of Pakistan. *Theor. Appl. Climatol.* **2019**. [CrossRef]
8. Ahmed, K.; Shahid, S.; Chung, E.-S.; Wang, X.-J.; Harun, S.B. Climate Change Uncertainties in Seasonal Drought Severity-Area-Frequency Curves: Case of Arid Region of Pakistan. *J. Hydrol.* **2019**. [CrossRef]
9. Taormina, R.; Chau, K.-W.; Sivakumar, B. Neural network river forecasting through baseflow separation and binary-coded swarm optimization. *J. Hydrol.* **2015**, *529*, 1788–1797. [CrossRef]
10. Sa'adi, Z.; Shahid, S.; Ismail, T.; Chung, E.-S.; Wang, X.-J. Trends analysis of rainfall and rainfall extremes in Sarawak, Malaysia using modified Mann–Kendall test. *Meteorol. Atmos. Phys.* **2017**, 1–15. [CrossRef]
11. Ahmad, I.; Tang, D.; Wang, T.; Wang, M.; Wagan, B. Precipitation Trends over Time Using Mann-Kendall and Spearman's rho Tests in Swat River Basin, Pakistan. *Adv. Meteorol.* **2015**, *2015*, 15. [CrossRef]
12. Asfaw, A.; Simane, B.; Hassen, A.; Bantider, A. Variability and time series trend analysis of rainfall and temperature in northcentral Ethiopia: A case study in Woleka sub-basin. *Weather Clim. Extremes* **2018**, *19*, 29–41. [CrossRef]
13. Meshram, S.G.; Singh, V.P.; Meshram, C. Long-term trend and variability of precipitation in Chhattisgarh State, India. *Theor. Appl. Climatol.* **2017**, *129*, 729–744. [CrossRef]
14. Schmidhuber, J.; Tubiello, F.N. Global food security under climate change. *Proc. Natl. Acad. Sci. USA* **2007**, *104*, 19703–19708. [CrossRef] [PubMed]
15. Ahmed, K.; Shahid, S.; Harun, S.B.; Wang, X.-J. Characterization of seasonal droughts in Balochistan Province, Pakistan. *Stoch. Environ. Res. Risk Assess.* **2015**, *30*, 747–762. [CrossRef]
16. Ahmed, K.; Shahid, S.; Nawaz, N. Impacts of climate variability and change on seasonal drought characteristics of Pakistan. *Atmos. Res.* **2018**, *214*, 364–374. [CrossRef]
17. Ezzine, H.; Bouziane, A.; Ouazar, D. Seasonal comparisons of meteorological and agricultural drought indices in Morocco using open short time-series data. *Int. J. Appl. Earth Obs. Geoinf.* **2014**, *26*, 36–48. [CrossRef]

18. Cigizoglu, H.; Bayazit, M.; Önöz, B. Trends in the maximum, mean, and low flows of Turkish rivers. *J. Hydrometeorol.* **2005**, *6*, 280–290. [CrossRef]
19. Ehsanzadeh, E.; Adamowski, K. Trends in timing of low stream flows in Canada: Impact of autocorrelation and long-term persistence. *Hydrol. Process.* **2010**, *24*, 970–980. [CrossRef]
20. Hamed, K.H. Trend detection in hydrologic data: The Mann–Kendall trend test under the scaling hypothesis. *J. Hydrol.* **2008**, *349*, 350–363. [CrossRef]
21. Kumar, S.; Merwade, V.; Kam, J.; Thurner, K. Streamflow trends in Indiana: Effects of long term persistence, precipitation and subsurface drains. *J. Hydrol.* **2009**, *374*, 171–183. [CrossRef]
22. Zhang, X.; Harvey, K.D.; Hogg, W.; Yuzyk, T.R. Trends in Canadian streamflow. *Water Resour. Res.* **2001**, *37*, 987–998. [CrossRef]
23. Gajbhiye, S.; Meshram, C.; Singh, S.K.; Srivastava, P.K.; Islam, T. Precipitation trend analysis of Sindh River basin, India, from 102-year record (1901–2002). *Atmos. Sci. Lett.* **2016**, *17*, 71–77. [CrossRef]
24. Meshram, S.G.; Singh, S.K.; Meshram, C.; Deo, R.C.; Ambade, B. Statistical evaluation of rainfall time series in concurrence with agriculture and water resources of Ken River basin, Central India (1901–2010). *Theor. Appl. Climatol.* **2018**, *134*, 1231–1243. [CrossRef]
25. Wu, C.L.; Chau, K.W. Rainfall–runoff modeling using artificial neural network coupled with singular spectrum analysis. *J. Hydrol.* **2011**, *399*, 394–409. [CrossRef]
26. Luković, J.; Bajat, B.; Blagojević, D.; Kilibarda, M. Spatial pattern of recent rainfall trends in Serbia (1961–2009). *Region. Environ. Chang.* **2014**, *14*, 1789–1799. [CrossRef]
27. Liuzzo, L.; Bono, E.; Sammartano, V.; Freni, G. Analysis of spatial and temporal rainfall trends in Sicily during the 1921–2012 period. *Theor. Appl. Climatol.* **2015**, 1–17. [CrossRef]
28. Wickramagamage, P. Spatial and temporal variation of rainfall trends of Sri Lanka. *Theor. Appl. Climatol.* **2015**, 1–12. [CrossRef]
29. Yaseen, Z.M.; Sulaiman, S.O.; Deo, R.C.; Chau, K.-W. An enhanced extreme learning machine model for river flow forecasting: State-of-the-art, practical applications in water resource engineering area and future research direction. *J. Hydrol.* **2019**, *569*, 387–408. [CrossRef]
30. Chau, K.-W. Use of Meta-Heuristic Techniques in Rainfall-Runoff Modelling. *Water* **2017**, *9*, 186. [CrossRef]
31. Salman, S.A.; Shahid, S.; Ismail, T.; Chung, E.-S.; Al-Abadi, A.M. Long-term trends in daily temperature extremes in Iraq. *Atmos. Res.* **2017**, *198*, 97–107. [CrossRef]
32. Salman, S.A.; Shahid, S.; Ismail, T.; Rahman, N.B.A.; Wang, X.; Chung, E.-S. Unidirectional trends in daily rainfall extremes of Iraq. *Theor. Appl. Climatol.* **2017**, 1–13. [CrossRef]
33. Shubbar, R.M.; Salman, H.H.; Lee, D.I. Characteristics of climate variation indices in Iraq using a statistical factor analysis. *Int. J. Climatol.* **2017**, *37*, 918–927. [CrossRef]
34. Yousuf, M.; Rapantova, N.; Younis, J. Sustainable Water Management in Iraq (Kurdistan) as a Challenge for Governmental Responsibility. *Water* **2018**, *10*, 1651. [CrossRef]
35. Abbas, N.; Wasimi, S.; Al-Ansari, N.; Nasrin Baby, S. Recent Trends and Long-Range Forecasts of Water Resources of Northeast Iraq and Climate Change Adaptation Measures. *Water* **2018**, *10*, 1562. [CrossRef]
36. Issa, I.; Al-Ansari, N.; Sherwany, G.; Knutsson, S. Trends and future challenges of water resources in the Tigris–Euphrates Rivers basin in Iraq. *Hydrol. Earth Syst. Sci. Discuss.* **2013**, *10*, 14617–14644. [CrossRef]
37. Khan, N.; Shahid, S.; Ismail, T.; Ahmed, K.; Nawaz, N. Trends in heat wave related indices in Pakistan. *Stoch. Environ. Res. Risk Assess.* **2018**, 1–16. [CrossRef]
38. Khan, N.; Shahid, S.; Ismail, T.B.; Wang, X.-J. Spatial distribution of unidirectional trends in temperature and temperature extremes in Pakistan. *Theor. Appl. Climatol.* **2018**. [CrossRef]
39. Preethi, B.; Mujumdar, M.; Kripalani, R.; Prabhu, A.; Krishnan, R. Recent trends and tele-connections among South and East Asian summer monsoons in a warming environment. *Clim. Dyn.* **2016**, 1–17. [CrossRef]
40. Nashwan, M.S.; Shahid, S. Spatial distribution of unidirectional trends in climate and weather extremes in Nile river basin. *Theor. Appl. Climatol.* **2018**, 1–19. [CrossRef]
41. Chandniha, S.K.; Meshram, S.G.; Adamowski, J.F.; Meshram, C. Trend analysis of precipitation in Jharkhand State, India. *Theor. Appl. Climatol.* **2017**, *130*, 261–274. [CrossRef]
42. Ezz-Aldeen, M.; Hassan, R.; Ali, A.; Al-Ansari, N.; Knutsson, S. Watershed Sediment and Its Effect on Storage Capacity: Case Study of Dokan Dam Reservoir. *Water* **2018**, *10*, 858. [CrossRef]
43. Hassan, R.; Al-Ansari, N.; Ali, S.S.; Ali, A.A.; Abdullah, T.; Knutsson, S. Dukan Dam Reservoir Bed Sediment, Kurdistan Region, Iraq. *Engineering* **2016**, *8*, 582–596. [CrossRef]

44. Pilesjo, P.; Al-Juboori, S.S. Modelling the effects of climate change on hydroelectric power in Dokan, Iraq. *Int. J. Energy Power Eng.* **2016**, *5*, 7–12. [CrossRef]
45. Willmott, C.J.; Robeson, S.M.; Feddema, J.J. Estimating continental and terrestrial precipitation averages from rain-gauge networks. *Int. J. Climatol.* **1994**, *14*, 403–414. [CrossRef]
46. Teegavarapu, R.S.; Chandramouli, V. Improved weighting methods, deterministic and stochastic data-driven models for estimation of missing precipitation records. *J. Hydrol.* **2005**, *312*, 191–206. [CrossRef]
47. Eischeid, J.K.; Pasteris, P.A.; Diaz, H.F.; PLantico, M.S.; Lott, N.J. Creating a serially complete, national daily time series of temperature and precipitation for the western United States. *J. Appl. Meteorol.* **2000**, *39*, 1580–1591. [CrossRef]
48. Wallis, J.R.; Lettenmaier, D.P.; Wood, E.F. A daily hydroclimatological data set for the continental United States. *Water Resour. Res.* **1991**, *27*, 1657–1663. [CrossRef]
49. Coulibaly, P.; Evora, N. Comparison of neural network methods for infilling missing daily weather records. *J. Hydrol.* **2007**, *341*, 27–41. [CrossRef]
50. Ali Ghorbani, M.; Kazempour, R.; Chau, K.-W.; Shamshirband, S.; Taherei Ghazvinei, P. Forecasting pan evaporation with an integrated artificial neural network quantum-behaved particle swarm optimization model: A case study in Talesh, Northern Iran. *Eng. Appl. Comput. Fluid Mech.* **2018**, *12*, 724–737. [CrossRef]
51. Dempster, A.P.; Laird, N.M.; Rubin, D.B. Maximum likelihood from incomplete data via the EM algorithm. *J. R. Stat. Soc. Ser. B Methodol.* **1977**, *39*, 1–38. [CrossRef]
52. McLachlan, G.; Krishnan, T. *The EM Algorithm and Extensions*; John Wiley & Sons: Hoboken, NJ, USA, 1997; Volume 382.
53. Ahmed, K.; Shahid, S.; Ali, R.O.; Harun, S.B.; Wang, X.-J. Evaluation of the performance of gridded precipitation products over Balochistan Province, Pakistan. *Desalination* **2017**, *79*, 73–86. [CrossRef]
54. Ahmed, K.; Shahid, S.; Ismail, T.; Nawaz, N.; Wang, X.-J. Absolute homogeneity assessment of precipitation time series in an arid region of Pakistan. *Atmósfera* **2018**, *31*, 301–316. [CrossRef]
55. Noor, M.; Ismail, T.; Chung, E.-S.; Shahid, S.; Sung, J. Uncertainty in Rainfall Intensity Duration Frequency Curves of Peninsular Malaysia under Changing Climate Scenarios. *Water* **2018**, *10*, 1750. [CrossRef]
56. Sen, P.K. Estimates of the regression coefficient based on Kendall's tau. *J. Am. Stat. Assoc.* **1968**, *63*, 1379–1389. [CrossRef]
57. Ahmed, K.; Shahid, S.; Chung, E.-S.; Ismail, T.; Wang, X.-J. Spatial distribution of secular trends in annual and seasonal precipitation over Pakistan. *Clim. Res.* **2017**, *74*, 95–107. [CrossRef]
58. Souvignet, M.; Laux, P.; Freer, J.; Cloke, H.; Thinh, D.Q.; Thuc, T.; Cullmann, J.; Nauditt, A.; Flügel, W.-A.; Kunstmann, H.; et al. Recent climatic trends and linkages to river discharge in Central Vietnam. *Hydrol. Process.* **2014**, *28*, 1587–1601. [CrossRef]
59. Wang, S.; Zhang, X.; Liu, Z.; Wang, D. Trend analysis of precipitation in the Jinsha River Basin in China. *J. Hydrometeorol.* **2013**, *14*, 290–303. [CrossRef]
60. Mann, H.B. Nonparametric Tests Against Trend. *Econometrica* **1945**, *13*, 245. [CrossRef]
61. Sonali, P.; Nagesh Kumar, D. Review of trend detection methods and their application to detect temperature changes in India. *J. Hydrol.* **2013**, *476*, 212–227. [CrossRef]
62. Salman, S.A.; Shahid, S.; Ismail, T.; Ahmed, K.; Chung, E.-S.; Wang, X.-J. Characteristics of Annual and Seasonal Trends of Rainfall and Temperature in Iraq. *Asia-Pacif. J. Atmos. Sci.* **2019**. [CrossRef]
63. Hassan, R.; Al-Ansari, N.; Ali, A.A.; Ali, S.S.; Knutsson, S. Bathymetry and siltation rate for Dokan Reservoir, Iraq. *Lakes Reserv. Sci. Policy Manag. Sustain. Use* **2017**, *22*, 179–189. [CrossRef]